Microwave spectrum of benzene·SO_2: Barrier to internal rotation, structure, and dipole moment

Amine Taleb-Bendiab, Kurt W. Hillig II, and Robert L. Kuczkowski
Department of Chemistry, The University of Michigan, Ann Arbor, Michigan 48109-1055

(Received 30 January 1992; accepted 29 May 1992)

The microwave spectrum of the benzene·SO_2 complex was observed with a pulsed beam Fourier-transform microwave spectrometer. The spectrum was characteristic of an asymmetric-top with *a*- and *c*-dipole selection rules. In addition to the rigid-rotor spectrum, many other transitions were observed. The existence of a rich spectrum arose from torsional–rotation interactions from nearly free internal rotation of benzene about its C_6 axis. Transitions from torsional states up to $m=\pm 5$ were observed. The principal-axis method (PAM) internal rotation Hamiltonian with centrifugal distortion was used to assign the spectrum. Assuming six-fold symmetry for the internal rotation potential, the barrier height was determined as $V_6=0.277(2)$ cm^{-1}. The spectrum of $C_6D_6\cdot SO_2$ was also assigned. Analysis of the moments of inertia indicated that the complex has a stacked structure. The distance R_{cm} separating the centers of mass of benzene and SO_2, as well as the tilt angles of the benzene and SO_2 planes relative to R_{cm} were determined. The values obtained were $R_{cm}=3.485(1)$ Å, $\theta_{C_6H_6}=\pm 12(1)°$ and $\theta_{SO_2}=44(6)°$. While SO_2 is certainly tilted with the sulfur end towards benzene, the sign of the benzene tilt angle could not be unambiguously determined. The dipole moment of $C_6H_6\cdot SO_2$ was determined as $\mu_a=1.691(2)$ D, $\mu_c=1.179(2)$ D, and $\mu_T=2.061(2)$ D.

I. INTRODUCTION

The interaction between SO_2 and benzene in the condensed phase has been investigated for several decades.[1–4] From these studies it was inferred that SO_2 and benzene form a 1:1 complex, and that SO_2 interacts with the π system of benzene. However, detailed structural data have not been available. A few years ago, Grover *et al.* measured the dissociation energy (4.4 kcal mol^{-1}) of the gas-phase benzene·SO_2 complex using a photoionization technique.[5] More recently, we have reported the rigid-rotor microwave spectrum of benzene·SO_2 using a Fourier-transform microwave (FTMW) spectrometer.[6] The complex was shown to have a stacked configuration with SO_2 over the aromatic ring. However, numerous unassigned transitions were observed in the spectrum of the normal species. These additional transitions were suggestive of an internal rotation in the complex. Experimental evidence of internal rotation has also been found in two other benzene complexes, benzene·H_2O[7,8] and benzene·N_2,[9,10] and an internal rotation about the benzene C_6 axis was proposed. Solid-state nuclear magnetic resonance (NMR) studies of a series of benzene-containing complexes, including benzene·SO_2, have also shown evidence of internal rotation about the C_6 axis.[11]

In this paper, we report further analysis of the microwave spectrum of benzene·SO_2 using a FTMW spectrometer. We have been able to assign the many additional transitions to a model with an internal rotation of benzene about its C_6 axis using the principal-axis method (PAM) Hamiltonian. We have also assigned the internal rotation perturbed microwave spectrum of the fully deuterated species using the PAM Hamiltonian. In addition to the determination of the barrier to internal rotation, the assignment of the spectra was very helpful in obtaining rigid-rotor constants from which internal rotation effects were removed, and information on the tilt angle of benzene. These rigid-rotor constants, combined with data from spectral assignments of the ^{18}O species, have allowed us to determine a more detailed geometry for the complex.

II. EXPERIMENT

The microwave spectrum of benzene·SO_2 was observed in a Balle–Flygare FTMW spectrometer with a pulsed nozzle source.[12] A mixture of ~1% C_6H_6, 1% SO_2, and 98% Ne maintained at a pressure of 1–2 atm was employed to generate the spectrum. The transitions had full widths at half-maximum of ~15–30 kHz and the frequency measurement accuracy is estimated to be 4 kHz (unless otherwise stated).

The spectrometer was equipped with steel mesh plates for the measurement of Stark effects.[13] The $2_{02}\leftarrow 1_{11}$ transition of SO_2 was used as an electric field calibration standard [$\mu(SO_2)=1.633\,05$ D[14]]. Stark shifts were measured at electric field values between 0 and 600 V/cm.

The spectra of the isotopically substituted species were observed in enriched samples. Benzene-d_6 (99.5% enrichment, Aldrich Chemical Co.) was used without dilution. $S^{18}O_2$ (99% enrichment, Alfa Products) was used without dilution to assign the benzene·$S^{18}O_2$ spectrum. The spectrum of the benzene·$S^{16}O^{18}O$ species was observed starting with a 50%–50% mixture of $S^{16}O_2$ and $S^{18}O_2$, which equilibrates in our glass sample bulbs to form a statistical 2:1:1 mixture of $S^{16}O^{18}O$:$S^{16}O_2$:$S^{18}O_2$.

 0021-9606/92/172996-11$006.00 © 1992 American Institute of Physics

TABLE I. Ground torsional state ($m=0$) spectroscopic constants of benzene·SO_2.[a]

	$C_6H_6 \cdot SO_2$	$C_6D_6 \cdot SO_2$	$C_6H_6 \cdot S^{18}O_2$	$C_6H_6 \cdot S^{18}OO$
A'/MHz	9031.936(3)[b]	8949.707(3)	8088.525(4)	8539.9(18)
B'/MHz	963.9484(6)	907.9082(4)	931.624(1)	947.210(2)
C'/MHz	892.568(1)	845.0201(6)	856.391(2)	873.966(2)
D_J/kHz	0.754(7)	0.616(4)	0.70(1)	0.72(1)
D_{JK}/kHz	19.4(3)	16.9(2)	17.2(4)	20.5(1)
d_1/kHz	−0.058(4)	−0.048(3)	−0.037(11)	−0.046(14)
H_{JK}/kHz	0.014(3)	···	···	···
H_{KJ}/kHz	−0.62(6)	−0.45(4)	−0.47(10)	···
n[c]	28	20	13	11
$\Delta\nu^d_{rms}$/kHz	6	3	4	4

[a]The spectroscopic constants are determined using Watson S-reduced semirigid-rotor Hamiltonian with I^r representation (Ref. 26).
[b]The uncertainties are 1σ.
[c]Number of transitions.
[d]$\Delta\nu=\nu_{obs}-\nu_{calc}$.

III. RESULTS AND ANALYSIS

A. Spectral assignments

1. $C_6H_6 \cdot SO_2$

In an earlier report,[6] we presented initial results on benzene·SO_2, where 27 a- and c-dipole (R- and Q-branch) transitions of the normal species were assigned to a semirigid-rotor Hamiltonian. The spectrum was characteristic of a near-prolate asymmetric-top ($\kappa=-0.98$). We have refit these transitions plus one additional transition using two S-reduction sextic constants H_{JK} and H_{KJ} instead of the d_2 quartic constant used in Ref. 6. The $(\nu_{obs}-\nu_{calc})_{rms}$ of the fit for these lines was improved from 12 kHz[6] down to 6 kHz. The effective rotational constants and centrifugal distortion constants derived from the fit are listed in Table I. In addition, as mentioned in the earlier publication,[6] the spectrum was crowded by transitions which did not follow the same pattern. The majority of these transitions displayed a first-order Stark effect, whereas those assigned to the semirigid-rotor Hamiltonian had second-order Stark effects. Several of the transitions with first-order Stark effects formed recurring series in each J region of the spectrum.

Since the microwave spectrum of benzene·SO_2 contains many more transitions than the rigid-rotor Hamiltonian predicts, it is apparent that the complex undergoes some kind of internal motion(s). Some likely internal motions that could occur in benzene·SO_2 are rotation of SO_2 about its C_2 axis, an inversionlike motion of SO_2, the rotation of benzene about any of its C_2 axes or about its C_6 axis. The rotation of SO_2 about its symmetry axis would lead to a splitting of the rotational states into doublets, but only one substate would be present because oxygen has a nuclear spin of zero. Thus this motion cannot explain the existence of so many additional transitions, and consequently it can be ruled out. The inversionlike motion corresponds to a rotation of SO_2 about its a axis, which lies in the SO_2 plane and is perpendicular to the C_2 axis. If the benzene plane is tilted, this motion is simultaneously followed by a readjustment of this plane. The inversionlike motion is also accompanied by a change of direction of the dipole moment component along the c axis of the complex ($\mu_c \leftrightarrow -\mu_c$), causing c-dipole transitions to be shifted from their rigid-rotor pattern. The fact that both a- and c-type transitions were assigned to a semirigid-rotor Hamiltonian eliminates the possibility that SO_2 undergoes an inversionlike motion. The internal rotation of benzene about any of its C_2 axes is very improbable due to steric effects. In addition, the rotation about the C_2 axis would only lead to a doubling of each rigid-rotor transition which has not been observed. The internal rotation of benzene about its C_6 axis perpendicular to the aromatic ring is left as the likely motion that can explain the rich microwave spectrum for benzene·SO_2.

Assuming that the internal rotation of benzene about its C_6 axis is the motion that accounts for splittings in the spectrum, and based on the general conformation of benzene·SO_2[6] (see below), there are six equivalent frameworks (assuming a plane of symmetry) which corresponds to a rotation of benzene about the C_6 axis by steps of 60°. Therefore, the torsional–rotational energy levels can be classified in the permutation-inversion (PI) group isomorphic to the C_{6v} (or D_6) point group. Using the group theory method outlined by Longuet–Higgins[15] and Bunker,[16] we calculated the nuclear spin statistical weights for the various states of $C_6H_6 \cdot SO_2$. The results are summarized in Table II. An inspection of the statistical weights in Table II for $C_6H_6 \cdot SO_2$ shows that no levels are expected to be missing. Furthermore, in a given torsional level all of the rotational states have equal spin weights.

As seen from symmetry considerations, the internal rotation of benzene about the C_6 axis shows the existence of doubly degenerate torsional levels such as $m=\pm 1$ and ± 2. This explains the occurrence of transitions with the first-order Stark effect. The fact that several second-order Stark effect transitions of benzene·SO_2 have been fit to a semirigid-rotor Hamiltonian, suggests that these transitions are associated with the nondegenerate ground torsional state ($m=0$). Also, the observed transitions with a first-order Stark effect were more intense than those following a rigid-rotor pattern ($m=0$) which is in agreement with spin weights (see Table II). Moreover, many molecules with a very low sixfold internal rotation barrier also displayed a very dense spectrum.[17–22] Hence, benzene·SO_2 most likely exhibits tunneling perturbations from a low barrier to internal rotation. From the conformation of this complex[6] the torsional potential function is likely to have sixfold symmetry.

Based on the above observations, a prediction of the torsional–rotational spectrum of the $C_6H_6 \cdot SO_2$ was made using the PAM internal rotation Hamiltonian, written as follows:[23]

$$\mathscr{H}=AP_a^2+BP_b^2+CP_c^2+D_{ac}(P_aP_c+P_cP_a) -2(Q_aP_a+Q_cP_c)p+Fp^2+\tfrac{1}{2}V_6(1-\cos 6\alpha), \quad (1)$$

where

$$A=A_r+F\rho_a^2,\ B=B_r,\ C=C_r+F\rho_c^2,$$

TABLE II. Spin statistical weights for $C_6H_6 \cdot SO_2$ and $C_6D_6 \cdot SO_2$.

			$C_6H_6 \cdot SO_2$ $\Gamma^H_{spin}=13A_1+A_2+7B_1+3B_2+9E_1+11E_2$				$C_6D_6 \cdot SO_2$ $\Gamma^D_{spin}=92A_1+38A_2+73B_1+46B_2+116E_1+124E_2$			
			Γ_{rot}				Γ_{rot}			
			A_1		A_2		A_1		A_2	
$\lvert m \rvert$	Y^a	Γ_{tors}	(B_1+B_2)		(B_1+B_2)		(A_1+A_2)		(A_1+A_2)	
0	0	A_1	7	3	3	7	92	38	38	92
1	1	E_1	11	11	11	11	116	116	116	116
2	2	E_2	9	9	9	9	124	124	124	124
		B_1	13	1	1	13	73	46	46	73
3	3	+								
		B_2	1	13	13	1	46	73	73	46
4	2	E_2	9	9	9	9	124	124	124	124
5	1	E_1	11	11	11	11	116	116	116	116
		A_2	3	7	7	3	38	92	92	38
6	0	+								
		A_1	7	3	3	7	92	38	38	92

[a]See definition of Y in Sec. III A.

$$D_{ac}=F\rho_a\rho_c,\ Q_a=F\rho_a,\ Q_c=F\rho_c,$$

$$F=F_\alpha[1-\rho_a\cos(\theta_a)-\rho_c\cos(\theta_c)]^{-1},$$

$$\rho_a=\frac{A_r}{F_\alpha}\cos(\theta_a),\ \rho_c=\frac{C_r}{F_\alpha}\cos(\theta_c).$$

P_a, P_b, and P_c are the projections of the total angular momentum onto the principal axes, a, b, and c (I^r representation); p is the angular momentum of the internal rotor, α is the internal rotation angle, and V_6 is the barrier height; A_r, B_r, and C_r are the rigid-rotor rotational constants in the principal axes; F_α is inversely proportional to the moment of inertia (I_α) of the internal rotor; θ_a (θ_c) is the angle between the internal rotor axis (C_6 axis of benzene), and the a (c) axis. The convention will be taken that θ_a varies between 0° and 90°, and that θ_c is its complementary angle. The implicit assumption that benzene is the internal rotor and SO_2 is the frame is a reasonably good approximation because an examination of the A' constant of the normal species (see Table I) shows that it falls between the $B=10\,318$ MHz and $C=8800$ MHz constants of free SO_2,[24] instead of ~2240 MHz expected from a structural model. As observed in other sixfold internal rotors,[17–22,25] the fact that the A' constant is close to the rotational constants of free SO_2, indicates that SO_2 behaves like a frame.

The Hamiltonian matrix of $\mathscr{H}$ is constructed using $|JKM\rangle \cdot |m\rangle$ as a basis set, where $|JKM\rangle$ are symmetric-top wave functions and $|m\rangle$ are free rotor wave functions. Since the free rotor quantum number m has no finite limits, the Hamiltonian matrix is infinite. However, a truncation of the matrix at a given m value can occur when a desirable energy convergence is met. Since a sixfold symmetry potential function is applied [see Eq. (1)], the Hamiltonian matrix may be factored into six submatrices which are arbitrarily labeled by the symbol Y. The symbol equals the lowest positive value of m, that is, $Y=0$, 1, 2, 3, 4, and 5. The two submatrices $Y=0$ and 3 are nondegenerate, whereas the other ones are doubly degenerate. The submatrices $Y=1$ and 5 will lead to identical eigenvalues, and likewise for $Y=2$ and 4. Hence, only the labels $Y=0$, 1, 2, and 3 will be used. The symmetry species associated with each label Y are listed in Table II.

In the first stage of calculating the torsional–rotational spectrum of $C_6H_6 \cdot SO_2$, the effective rotational constants were held fixed at the values shown in Table I, the barrier to internal rotation V_6 was set to zero, and the C_6 axis of benzene aligned with the a axis ($\theta_a=0°$ and $\theta_c=90°-\theta_a$) of the complex. With these conditions, no pattern was developed that could reproduce the observed spectrum for $m>0$. We increased the barrier V_6 from zero while the other parameters remained unchanged, but the predictions were only slightly sensitive. However, when the tilt angle θ_a was increased from zero by steps of 5° while the barrier was set to zero and the other parameters held fixed, the predicted transitions were strongly affected as shown in Table III for several $J=5\leftarrow4$ a-dipole transitions. A resemblance started to develop between the calculated and the observed a-dipole spectra for θ_a around 15°, where many transitions arising from torsional states up to $m=\pm3$ were matched within a few MHz (see Table III). The perturbation caused in the torsional–rotational spectrum by the change of the angles θ_a and θ_c shows up in the coupling terms Q_iP_ip ($i=a$ and c). Unlike the ground torsional state, the excited torsional states tend to be tremendously affected by these coupling terms depending on the relative magnitude of Q_i.

Some a-dipole transitions which were matched to the $m=\pm3$ torsional state were observed as doublets split by 60–500 kHz. This shows that a nonzero V_6 barrier is definitely present. Similar splitting in the $m=\pm3$ transitions was also observed in all other sixfold symmetry molecules.[17–22,25] Although not definitive evidence, the occurrence of a sixfold potential favors the presence of an ac-plane of symmetry in benzene·SO_2. The assignment of $m>0$ c-dipole transitions was achieved by setting the Hamiltonian parameters from Eq. (1) to values that led to the closest agreement between the predicted and the observed a-dipole torsional–rotational transitions. Several ob-

TABLE III. The effect of the tilt of the C_6 axis on a-dipole $m>0$ transitions for $J=5\leftarrow 4$.[a]

		Calc. freq.[b]				
		$\theta_a^c=0.0°$	5.0°	10.0°	14.3°	
$\lvert m\rvert$	$J'K_a't'-J''K_a''t''$					Obs. freq.[b]
1	5 1 1−4 1 1	9272.950	9265.120	9241.874	9210.045	9209.688
2	5 2 1−4 2 1	9273.444	9237.506	9139.988	9022.174	9020.991
3	5 3 1−4 3 1	9274.250	9166.510	8929.550	8690.567	8688.666

[a]See Sec. III A for the definition of the transition labels.
[b]The frequencies are in MHz.
[c]The angle θ_c is also varied following the relationship $\theta_c=90°-\theta_a$.

served $m>0$ c-dipole Q-branch transitions were compatible with Stark effect measurements. Confirmation of the whole assignment was accomplished from measurements of additional transitions in which most were found no more than a few MHz from their respective predictions. The complete set of measured transitions of $C_6H_6\cdot SO_2$ is given in Table IV. The transitions are grouped in their respective sub-blocks $Y=0$, 1, 2, and 3. Although m is no longer a good quantum number, it is still a useful label for the torsional states, therefore, it is used in Table IV. Transitions arising from torsional levels up to $m=\pm 4$ and ± 5 were observed (see Table IV). Since some transitions arising from the $m=\pm 3$ torsional states were split into doublets due to a nonzero barrier V_6, these states are further defined by a + or − sign added as a superscript to $|m|=3$. This notation is based on the sign of the following wave function combination:[23]

$$|J,K,M,m=3^{\pm}\rangle=|J,+K,M,m=+3\rangle \pm|J,-K,M,m=-3\rangle, \quad (2)$$

whose coefficients are the largest in the corresponding eigenvector. For the unsplit $m=\pm 3$ transitions, the ± sign is used. Rotational energy levels associated with each torsional state m are generally labeled with the usual asymmetric rotor notation JK_aK_c. This notation can still be used for transitions arising from the ground torsional state. However, it can be misleading for the transitions associated

TABLE IV. Torsional–rotational transitions (in MHz) of benzene·SO_2.

$Y=0$		$C_6H_6\cdot SO_2$		$C_6D_6\cdot SO_2$		$Y=1$		$C_6H_6\cdot SO_2$		$C_6D_6\cdot SO_2$	
$\lvert m\rvert$	$J'K_a't'-J''K_a''t''$	ν_{obs}	$\Delta\nu^a$	ν_{obs}	$\Delta\nu^a$	$\lvert m\rvert$	$J'K_a't'-J''K_a''t''$	ν_{obs}	$\Delta\nu^a$	ν_{obs}	$\Delta\nu^a$
0	1 1 3−0 0 1	9 995.844	0.000			1	2 2 2−1 1 1	10 222.685	−0.031		
0	2 1 3−1 0 1	11 923.633	−0.007			1	3 2 2−2 1 1	12 110.695	−0.028		
0	3 1 3−2 0 1	13 887.213	−0.006	13 520.549	0.012	1	4 2 2−3 1 1	14 008.007	−0.020		
0	1 1 2−1 0 1	8 067.952	0.004			1	1 0 2−1 1 1	9 721.324	0.045		
0	2 1 2−2 0 1	7 996.963	−0.001			1	2 0 3−2 1 1	9 751.750	0.030		
0	3 1 2−3 0 1	7 891.368	−0.009	7 885.987	0.010	1	3 0 3−3 1 1	9 803.795	0.011		
0	4 1 2−4 0 1	7 752.239	−0.015	7 763.025	0.004	1	4 0 3−4 1 1	9 884.913	−0.006		
0	5 1 2−5 0 1	7 581.003	−0.019	7 611.405	−0.005	1	5 0 3−5 1 1	10 004.480	−0.022		
0	6 1 2−6 0 1	7 379.449	−0.014	7 432.517	−0.016	1	6 0 3−6 1 1	10 173.097	−0.033		
0	4 0 1−3 0 1	7 421.159	−0.004			1	4 1 1−3 1 1	7 372.874	−0.007		
0	4 1 2−3 1 2	7 282.031	−0.009			1	4 2 2−3 2 2	7 429.963	−0.001		
0	4 1 3−3 1 3	7 567.507	−0.005			1	4 0 3−3 0 3	7 453.988	−0.028		
0	4 2 4−3 2 4	7 424.820	−0.058			1	4 3 4−3 3 4	7 430.423	−0.067		
0	5 0 1−4 0 1	9 272.781	0.003	8 756.995	0.014	1	5 1 1−4 1 1	9 209.688	−0.002	8 704.092	0.007
0	5 1 2−4 1 2	9 101.545	−0.001	8 605.374	0.005	1	5 2 2−4 2 2	9 276.515	0.014	8 759.326	0.017
0	5 1 3−4 1 3	9 458.347	0.010	8 919.734	0.012	1	5 0 3−4 0 3	9 329.253	−0.020	8 803.950	−0.016
0	5 2 4−4 2 4	9 280.306	−0.057	8 762.771	−0.047	1	5 3 4−4 3 4	9 289.175	−0.064		
0	5 2 5−4 2 5	9 289.735	−0.051	8 770.107	−0.055	1	5 1 5−4 1 5	9 287.499	0.011		
0	6 0 1−5 0 1	11 121.964	0.011	10 504.196	0.020	1	6 1 1−5 1 1	11 042.283	0.003	10 437.682	0.013
0	6 1 2−5 1 2	10 920.408	0.014	10 325.307	0.008	1	6 2 2−5 2 2	11 117.167	0.036	10 498.608	0.031
0	6 1 3−5 1 3	11 348.482	0.032	10 702.475	0.027	1	6 0 3−5 0 3	11 210.901	−0.007	10 578.138	−0.011
0	6 2 4−5 2 4	11 135.314	−0.045	10 514.487	−0.050	1	6 3 4−5 3 4	11 148.680	−0.057	10 525.214	−0.044
0	6 2 5−5 2 5	11 151.807	−0.030	10 527.333	−0.046	1	6 1 5[b]−5 1 5	11 146.272	0.039	10 523.328	−0.011
0	7 0 1−6 0 1	12 968.239	0.026	12 249.119	0.027	1	7 1 1−6 1 1	12 869.923	0.017	12 167.393	0.016
0	7 1 2−6 1 2	12 738.503	0.042	12 044.631	0.015	1	7 2 2−6 2 2	12 952.412	0.068	12 233.005	0.046
0	7 1 3−6 1 3	13 237.764	0.066	12 484.549	0.050	1	7 0 3−6 0 3	13 098.435	0.016	12 357.581	0.005
0	7 2 4−6 2 4	12 989.747	−0.022	12 265.754	−0.041	1	7 3 4−6 3 4			12 281.178	−0.036
0	7 2 5−6 2 5	13 016.103	0.005	12 286.282	−0.039	1	7 1 5[b]−6 1 5[b]			12 278.583	0.000
						5	7 6[c] 6[b]−6 6[c] 6[b]	11 312.109	0.001	10 760.373	0.000

TABLE IV. (*Continued.*)

$Y=2$						$Y=3$						
2	1 1 1−2 2 1	7 635.974	−0.084			3^+	4 2 5−4 3 1	13 654.853	−0.018			
2	3 3 2−2 2 1	10 589.044	0.029	10 401.339[d]	0.010	3^-	4 2 6−4 3 2	13 654.973	−0.022			
2	4 3 2−3 2 1	12 704.637	0.042	12 370.146[d]	0.030	3^+	5 2 5−5 3 1	14 331.893	−0.023			
2	5 3 2−4 2 1			14 402.040[d]	−0.033	3^-	5 2 6−5 3 2	14 332.184	−0.021			
2	2 1 2−2 2 1	11 367.001	0.055			3^+	4 2 5−3 2 3	7 493.028	−0.049			
2	3 1 3−3 2 1	11 549.265	0.025			3^-	4 2 6−3 2 4	7 493.093	−0.067			
2	4 1 3−4 2 1	11 795.289	−0.002			3^+	4 1 7−3 1 5	7 439.360	0.199			
2	5 1 3−5 2 1	12 107.445	−0.030			3^-	4 1 8−3 1 6	7 449.940	0.187			
2	6 1 3−6 2 1			12 104.162[d]	0.020	$3^\pm$	5 3 1−4 3 1	8 688.666	−0.052	8 258.734	−0.041
2	7 1 3−7 2 1			12 489.455[d]	−0.028	$3^\pm$	5 4 3−4 4 3	9 616.424	0.002		
2	4 2 1−3 2 1	7 218.759	−0.025			3^+	5 2 5−4 2 5	9 365.712	−0.051	8 837.606	−0.045
2	4 3 2−3 3 2	7 530.757	−0.009			3^-	5 2 6−4 2 6	9 365.877	−0.052	8 837.718	−0.072
2	4 1 3−3 1 3	7 464.781	−0.053			3^+	5 1 9−4 1 7	9 299.604[e]	0.274		
2	5 2 1−4 2 1	9 020.991	−0.023	8 544.230	−0.011	3^-	5 1 10−4 1 8	9 312.803[e]	0.235		
2	5 3 2−4 3 2	9 408.571	0.011	8 869.526	0.020	$3^\pm$	6 3 1−5 3 1	10 490.500	−0.035	9 957.363	−0.019
2	5 1 3−4 1 3	9 333.147	−0.051	8 808.591	−0.039	$3^\pm$	6 4 3−5 4 3	11 470.241	0.012	10 806.291	0.011
2	5 4 5−4 4 5	9 302.463	0.022			3^+	6 2 5−5 2 5	11 237.613	−0.038	10 604.251	−0.051
2	5 0 8−4 0 7	9 294.941	0.112	8 775.105	0.036	3^-	6 2 6−5 2 6	11 237.904	−0.036	10 604.487	−0.058
2	6 2 1−5 2 1	10 821.498	−0.016	10 249.228	−0.007	3^+	6 1 9−5 1 9	11 160.126[e]	0.359	10 534.905	0.147
2	6 3 2−5 3 2	11 283.656	0.037	10 638.864	0.038	3^-	6 1 10−5 1 10	11 175.939[e]	0.292	10 549.864	0.145
2	6 1 3−5 1 3	11 202.443	−0.042	10 572.734	−0.042	$3^\pm$	7 3 1−6 3 1	12 291.020	−0.005	11 657.331	−0.006
2	6 4 5[b]−5 4 5[b]	11 164.572	0.052	10 538.611	0.038	$3^\pm$	7 4 3−6 4 3	13 322.729	0.036	12 561.184	0.021
2	7 2 1−6 2 1	12 620.001	−0.004	11 952.334	0.003	3^+	7 2 5−6 2 5	13 108.220	−0.012	12 369.999	−0.050
2	7 3 2−6 3 2	13 155.778	0.071	12 405.989	0.055	3^-	7 2 6−6 2 6	13 108.677	−0.017	12 370.389	−0.049
2	7 1 3−6 1 3	13 072.395	−0.034	12 337.631	−0.041	3^+	7 1 9−6 1 9			12 291.389[e]	0.196
2	7 4 6−6 4 6			12 296.789	0.056	3^-	7 1 10−6 1 10			12 308.807[e]	0.167
4	6 4 4−5 4 4	10 009.284	−0.049								
4	6 5 6−5 5 6	11 738.929	−0.034								
4	6 3 7−5 3 7	11 286.757	0.065								
4	7 4 4−6 4 4	11 891.597	0.019	11 291.670	0.007						
4	7 3 7−6 3 7			12 420.294	−0.005						

[a]$\Delta\nu=\nu_{obs}-\nu_{calc}$ in MHz.
[b]The energy levels are interchanged for $C_6D_6\cdot SO_2$, therefore, numbers 5 and 6 should be exchanged for the label t.
[c]The $K_a=6$ level for this $m=5$ transition is strongly mixed with the $K_a=5$.
[d]These frequencies are estimated to be accurate to 50 kHz due to the deuterium quadrupole broadening.
[e]Transitions omitted from fitting analysis.

with the excited torsional states. In this work, we used a different notation for labeling these levels. This is JK_at (see Table IV), where J has its usual meaning and K_a is the value of K for a near-prolate asymmetric-top ($\kappa=-0.98$ for $C_6H_6\cdot SO_2$). The third index t represents the numbering of the energy levels within each Y subblock in order of increasing energy (i.e., $t=1$ corresponds to the lowest energy). This nomenclature is similar to that used by Langridge-Smith *et al.* in their analysis of the torsional–rotational spectrum of SiF_3BF_2.[22]

For $C_6H_6\cdot SO_2$ the torsional–rotational transitions (including $m=0$) listed in Table IV were least-squares fit to the PAM internal rotation Hamiltonian in Eq. (1). To account for the effects of centrifugal distortion, the following expression was added:

$$\mathscr{H}_{\text{dist.}}=-D_JP^4-D_{JK}P^2P_a^2+d_1P^2(P_+^2+P_-^2)$$
$$-D_{Jm}P^2p^2+D_{JKm}P^2P_a^2p^2$$
$$+2L_{Ja}P^2P_ap+L_{Kc}([P_a^2]P_ap+P_ap[P_a^2]), \quad (3)$$

where $P_\pm=P_b\pm iP_c$. These distortion parameters were derived employing the standard Hamiltonian similar to that introduced by Rohart.[18] The first three terms are the usual centrifugal distortions (Watson S-reduction[26]) associated with the overall rotation and the remaining terms are distortions associated with the internal rotation and its coupling with the overall rotation. These distortion terms, which were added empirically, are compatible with the time-reversal invariance requirement and they belong to the totally symmetric species of the C_{6v} (or D_6) point group.[27]

The resulting infinite Hamiltonian matrix, factored into $Y=0$, 1, 2, and 3, was diagonalized with the free rotor basis set truncated at $m=\pm 11$ for the benzene·SO_2 normal species. The moment of inertia of the internal top I_α was fixed at the value 177.0 amu Å^2 (I_c of free C_6H_6[28]). The fit of a total of 101 observed torsional–rotational transitions of $C_6H_6\cdot SO_2$ is given in Table IV. The spectroscopic constants obtained from the fit of the transitions of $C_6H_6\cdot SO_2$ are listed in Table V. The sum of the squares of the direction cosines should be equal to one [$\cos^2(\theta_a)+\cos^2(\theta_c)=1$], however, because of the large-amplitude vibrations in weakly bound complexes, this constraint is not necessarily maintained and was relaxed. Therefore, for $C_6H_6\cdot SO_2$ the tilt angles θ_a and θ_c were fit independently.

TABLE V. Spectroscopic constants for benzene·SO_2 derived using the internal rotation Hamiltonian.

	$C_6H_6 \cdot SO_2$	$C_6D_6 \cdot SO_2$
A/MHz	8976.43(5)[a]	8870.55(7)
B/MHz	963.950(4)	907.909(4)
C/MHz	949.495(5)	926.007(7)
D_J/kHz	0.73(2)	0.56(2)
D_{JK}/kHz	19.8(4)	17.2(3)
d_1/kHz	−0.10(3)	−0.10(3)
D_{Jm}/kHz	30.8(5)	25.7(4)
D_{JKm}/kHz	−0.078(18)	−0.036(24)
L_{Ja}/kHz	22.9(4)	19.5(4)
L_{Kc}/kHz	2.4(4)	1.5(4)
V_6/cm^{-1}	0.277(2)	0.294(2)
θ_a/deg.	14.2824(3)	14.9629(4)
θ_c/deg.	75.6478(4)	74.9702(5)
n[b]	101	66
$\Delta\nu^c_{rms}$/kHz	48	45
A_r^d/MHz	2238.753	1924.994
B_r/MHz	963.950	907.909
C_r/MHz	881.198	832.428
Q_a/MHz	8867.138	8778.837
Q_c/MHz	892.753	1018.996
D_{ac}/MHz	678.357	806.199
F/MHz	11669.614	11096.022

[a]The uncertainties are 1σ.
[b]Number of transitions.
[c]$\Delta\nu = \nu_{obs} - \nu_{calc}$.
[d]A_r, B_r, C_r, Q_a, Q_c, D_{ac}, and F are obtained after the fitting process from the varied parameters using the relationships in Eq. (1).

Because most of the $m>0$ transitions were very sensitive to the direction cosines, the angles θ_a and θ_c were very accurately determined as seen in Table V. The sum of the squared cosines $[\cos^2(\theta_a)+\cos^2(\theta_c)=1.0006]$ shows that the deviation from unity is very small. The centrifugal distortion constants as well as the barrier height V_6 determined from the fit are given in Table V. Fitting the angles θ_a and θ_c independently, and including various distortion parameters (listed in Table V), led to a fairly respectable rms error ($\Delta\nu_{rms}=48$ kHz) for the fit of transitions in Table IV. The constants A_r, B_r, C_r, Q_a, Q_c, and F listed in Table V were not fit but instead adjusted internally after each iteration based on the expressions in Eq. (1) relating them to the fitted parameters.

Torsional–rotational energy levels between 0–140 GHz are plotted in Fig. 1 for $J=4$ using the spectroscopic constants of the normal species from Table V. As shown in this figure, the rotational energy levels associated with the $m=0$ state follow the ordinary near-prolate asymmetric-top pattern where the regular order with respect to K_a is observed. However, this order is no longer respected for the excited torsional states, and it tends to vary between different J levels. The irregular order in the $m>0$ states is due mainly to the relatively large coupling constant Q_a. For the case of a nearly free internal rotation and $|K|>1$, the $Q_aK|m|$ term causes rotational levels for each of the K doublets to shift apart from each other with increasing $|m|$ and/or $|K|$ (or K_a). This explains the irregularity in the $m>0$ energy levels, hence the necessity of using the JK_at notation. Moreover, an inspection of the energy diagram in Fig. 1 shows that some levels from $m=\pm1$ are shuffled with those from $m=\pm5$ ($m=\pm1$ and ±5 belong to the same submatrix $Y=1$), and likewise for the levels from $m=\pm2$ and ±4. This is due to the closely packed torsional levels as a result of the involvement of a heavy internal top which leads to a small F ($E_{tor}\approx Fm^2$). Further splitting in the $m=\pm3$ states caused by the nonzero sixfold barrier is shown in Fig. 1, where the splitting is largest for the $K_a=0$ level and decreases as K_a increases.

2. $C_6D_6 \cdot SO_2$

The torsional–rotational spectrum of $C_6D_6 \cdot SO_2$ was also analyzed. The assigned ground torsional state ($m=0$) of this species was presented in an earlier publication.[6] As in the normal species the ground torsional state transitions were fit using the semirigid-rotor Hamiltonian. The derived spectroscopic constants are given in Table I. Here again the H_{KJ} constant was used instead of d_2 employed in the earlier fit, and H_{JK} was fixed to zero. The internal rotation Hamiltonian discussed above was also applied in the prediction of the excited m state transitions of $C_6D_6 \cdot SO_2$, and subsequently in the fit of the complete set of measured transitions including the $m=0$ lines. The Hamiltonian matrix was truncated at $m=\pm11$. The mo-

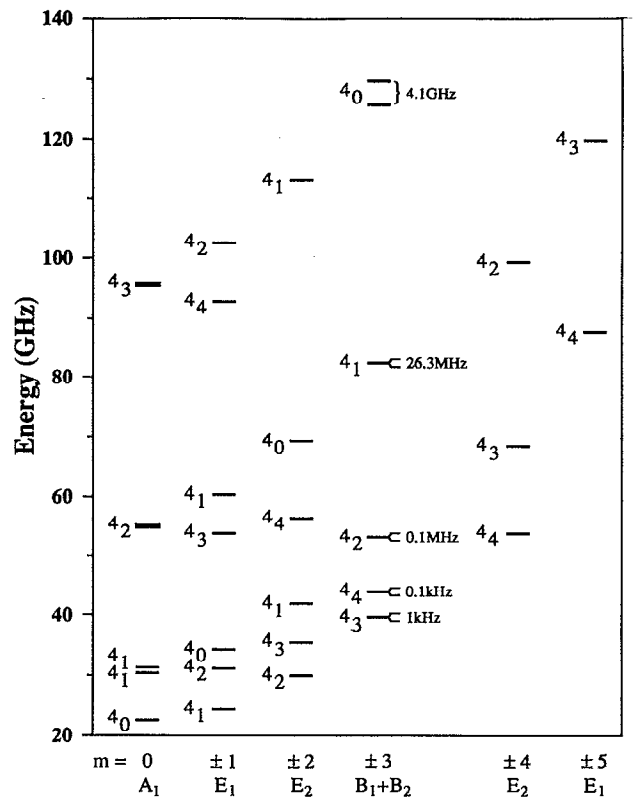

FIG. 1. Torsional–rotational energy levels of $C_6H_6 \cdot SO_2$ for $J=4$. The energy levels are grouped in six different columns with respect to the m torsional states. The subscript of the $J=4$ levels correspond to the K_a value. The label t defined in the text but not shown in this diagram can be determined from the ordering of the energy levels within each Y subblock. The magnitude of the splitting in the $m=\pm3$ state is given for each rotational level.

ment of inertia I_α of the internal top was fixed at 215 amu Å^2 (I_c of free C_6D_6). Since $C_6D_6 \cdot SO_2$ has the same symmetry as the normal species, this isotopic species belongs to the PI group, isomorphic with C_{6v} (or D_6). The spin weights were also derived for this species and are given in Table II. The assignment of transitions of $C_6D_6 \cdot SO_2$ was based on predictions aided by the results from the normal species. Although the assignment of $m>0$ a-type transitions was somewhat straightforward, difficulties arose in finding several $m>0$ c-type transitions even though they were expected to be as strong as those of $C_6H_6 \cdot SO_2$. This turned out to be caused by unresolved deuterium quadrupole splitting which leads to line broadening and a decrease in intensity for these particular transitions, necessitating extensive signal averaging. The complete set of observed transitions of $C_6D_6 \cdot SO_2$ is given in Table IV. The spectroscopic constants obtained from the fit of these transitions are listed in Table V. These constants in comparison with those obtained for the normal species do not show any irregularity, except that the B rotational constant is smaller than C; the rigid-rotor rotational constants must satisfy the conventional order, that is, $A_r > B_r > C_r$ as shown in Table V, and since benzene·SO_2 is only slightly asymmetric, this unusual order of B and C occurred. Finally, the small barrier height $V_6 = 0.28$ cm^{-1} for internal rotation is comparable for $C_6H_6 \cdot SO_2$ and $C_6D_6 \cdot SO_2$.

3. $C_6H_6 \cdot S^{18}O_2$ and $C_6H_6 \cdot S^{18}OO$

To shed some light on the relative orientation of SO_2, with respect to the line joining its center of mass to that of benzene, the ground torsional ($m=0$) spectra of the double-^{18}O and single-^{18}O isotopic species were assigned. The assigned transitions for both species are listed in Table VI, where the usual asymmetric rotor labels JK_aK_c are used. The spectroscopic constants derived from fitting the transitions in Table VI with a semirigid-rotor Hamiltonian are given in Table I. No attempt has been made to assign the excited torsional state transitions for these ^{18}O species. However, during the course of searching for the $m=0$ transitions, some additional ones were found which are most likely associated with the excited states. It is important to note that the spectrum of only one single-^{18}O species was found, indicating that the two oxygens are equivalent. Although, this does not confirm the existence of a plane of symmetry (ac-plane) in benzene·SO_2, it does show that the angle θ_b of the C_6 axis with respect to the b axis of the complex is equal to 90°.

B. Dipole moment

The Stark shifts for ten M components from four transitions were measured, as shown in Table VII. Since the transitions involved in the Stark measurements are only those arising from the $m=0$ state, the common JK_aK_c notation is sufficient. The second-order Stark coefficients were obtained from fits of $\Delta\nu$ vs $\mathscr{E}^2$. The observed coefficients are listed in Table VII. Plots of $\Delta\nu/\mathscr{E}^2$ vs $\mathscr{E}^2$ showed no significant curvature from nonsecond-order effects. The effective rotational constants were employed for the calculated Stark coefficients. Among these constants only A and C are contaminated by the internal rotation (since $\theta_b = 90°$). Therefore, the resultant dipole components will be those along the effective principal axes, which are rotated, in the ac-plane, by ~5° from the actual principal axes.[29] A least-squares fit of the observed coefficients, with μ_b fixed at zero, yielded a total dipole moment $\mu_T = 2.061(2)$ D with components $\mu_a = 1.691(2)$ D and $\mu_c = 1.179(2)$ D.

TABLE VI. The $m=0$ state rotational transitions (in MHz) for the ^{18}O isotopic species of benzene·SO_2.

	$C_6H_6 \cdot S^{18}O_2$		$C_6H_6 \cdot S^{18}OO$	
$J'_{K'_aK'_c} - J''_{K''_aK''_c}$	ν_{obs}	$\Delta\nu$[a]	ν_{obs}	$\Delta\nu$[a]
$1_{10}-0_{00}$	9020.113	3		
$2_{11}-1_{01}$	10883.265	−1		
$3_{12}-2_{02}$	12784.183	−2		
$4_{13}-3_{12}$	7301.007	2	7429.778	2
$5_{05}-4_{04}$	8927.937	2	9094.987	−2
$5_{15}-4_{14}$	8748.932	−2	8919.954	3
$5_{14}-4_{13}$	9124.998	1	9286.079	1
$5_{24}-4_{23}$			9103.535	−1
$5_{23}-4_{22}$	8949.435	−2	9114.072	−3
$6_{06}-5_{05}$	10706.872	−3	10908.012	−5
$6_{16}-5_{15}$	10496.969	2	10702.353	2
$6_{15}-5_{14}$	10948.134	−1	11141.609	3
$6_{25}-5_{24}$	10723.905	−6	10923.092	4
$6_{24}-5_{23}$	10744.526	7	10941.510	−3

[a] $\Delta\nu = \nu_{obs} - \nu_{calc}$ in kHz.

C. Structure

The gross configuration of benzene·SO_2 was initially determined,[6] where the molecular planes of benzene and SO_2 are stacked one above the other and their centers of mass are separated by a distance R_{cm} of 3.48(2) Å. This initial conformation was derived from analyses of the effective rotational constants (A' not included) of $C_6H_6 \cdot SO_2$ and $C_6D_6 \cdot SO_2$. Determination of tilt angles θ_1 and θ_2 of SO_2 and the benzene plane, respectively, relative to R_{cm} (see Fig. 2), however, was ambiguous because additional

TABLE VII. Stark coefficients for the ground internal rotation state ($m=0$) transitions and dipole moment of benzene·SO_2.

Transition	$\lvert M \rvert$	$\Delta\nu/\mathscr{E}^2$ [a]	obs.-calc.
$3_{13}-3_{03}$	2	−0.259	0.002
	3	−0.728	−0.001
$4_{04}-3_{03}$	1	−0.252	−0.002
	2	−0.159	−0.001
$5_{05}-4_{04}$	1	0.738	0.002
	2	0.638	−0.003
	3	0.479	−0.002
	4	0.257	0.000
$5_{14}-4_{13}$	1	0.236	0.001
	2	0.158	0.000
	$\lvert\mu_a\rvert = 1.691(2)$ D [b]		
	$\lvert\mu_c\rvert = 1.179(2)$ D		
	$\lvert\mu_T\rvert = 2.061(2)$ D		

[a] Observed Stark coefficients in units of 10^{-4} MHz/(V/cm)^2.
[b] The uncertainties are 2σ.

data from suitable isotopic species were lacking at that time and contamination of the rotational constants from the internal rotation was not removed. Until the internal rotation problem was solved, estimation of the effects of this motion on each rotational constant was impossible.

The rigid-rotor (or unperturbed) rotational constants A_r, B_r, and C_r for $C_6H_6 \cdot SO_2$ and $C_6D_6 \cdot SO_2$, derived from spectral assignments, are given in Table V. Even though the assignment of torsional–rotational spectra of the ^{18}O isotopic species was not undertaken, the rigid-rotor rotational constants of $C_6H_6 \cdot S^{18}O_2$ and $C_6H_6 \cdot S^{18}OO$ can still be obtained by using the relationships in Eq. (1), the internal rotation results from the normal species, and the ^{18}O data in Table I. Therefore, the rigid-rotor rotational constants which are more reliable for structural analyses are employed throughout the remainder of this section.

The planar moment of inertia of the normal species, $P_{bb}=1/2(I_a+I_c-I_b)=137.44$ amu Å^2, is nearly equal to the sum of P_{aa} of free SO_2 and P_{aa} (or P_{bb}) of free benzene ($49.05+88.74=137.79$ amu Å^2).[24,28] This confirms the stacked configuration where the molecular planes of each subunit are perpendicular to the *ac*-plane of benzene·SO_2. The existence of only one assigned single-^{18}O species serves as further support of this conclusion. This is also compatible with the occurrence of *a*- and *c*-dipole moment selection rules.

The equilibrium torsional angle of the SO_2 relative to the benzene is indeterminable from the available data, hence it is fixed at an arbitrary position. In this work, it is chosen so that the C_2 axis of SO_2 is projected on the line joining two carbons diagonally opposite. If the geometries of SO_2 and benzene are assumed to be unperturbed upon complexation,[28] then the three structural parameters R_{cm}, θ_1, and θ_2 (see Fig. 2) can be determined. These three parameters can be derived from least-squares fits of the rigid-rotor moments of inertia of $C_6H_6 \cdot SO_2$, $C_6D_6 \cdot SO_2$, $C_6H_6 \cdot S^{18}O_2$, and $C_6H_6 \cdot S^{18}OO$. Information on the magnitude, but not the sign, of the tilt angle θ_2 (proportional to θ_a) of benzene was in fact extracted from torsional–rotational spectral assignments (see Table V). Due to the symmetry of benzene, the direction of the tilt angle θ_2 is ambiguous, therefore, leading to two fits dependent on the initial orientation with respect to this angle. These two fits labeled I and II yielded structural parameters which are given in Table VIII and the corresponding conformations are shown in Fig. 2. The value of $R_{cm}=3.485(1)$ Å obtained from fits I and II is in agreement with that obtained in the earlier report [$R_{cm}=3.48(2)$ Å],[6] although more

TABLE VIII. Structural parameters for benzene·SO_2 from least-squares fits using A_r, B_r, and C_r of all isotopic species; angles θ_a and θ_c, dipole moment components and coordinates of oxygens calculated from the least-squares fits and the Kraitchman analysis.

	Least-squares		
	I	II	Kraitchman[a]
R_{cm}/Å	3.485(1)[b]	3.485(1)	
θ_1/deg	46.1(58)	42.5(58)	
θ_2/deg	−11.2(10)	+11.8(11)	
ΔI_{rms}/amu Å^2 [c]	0.29	0.32	
θ_a/deg	14.70	14.06	
θ_c[d]/deg	75.30	75.94	
$\lvert\mu_a\rvert$/D	1.202	1.161	
$\lvert\mu_c\rvert$/D	1.106	1.149	
$\lvert a(O)\rvert$/Å	2.178	2.170	2.132
$\lvert b(O)\rvert$/Å	1.235	1.235	1.249
$\lvert c(O)\rvert$/Å	0.128	0.329	0.292

[a]Using single-^{18}O isotopic species data. The double-substitution coordinates (double-^{18}O data) are $\lvert a(O)\rvert=2.141$, $\lvert b(O)\rvert=1.236$, and $\lvert c(O)\rvert=0.275$.
[b]The uncertainties are 2σ.
[c]$\Delta I=I_{obs}-I_{calc}$.
[d]$\theta_c=90°-\theta_a$.

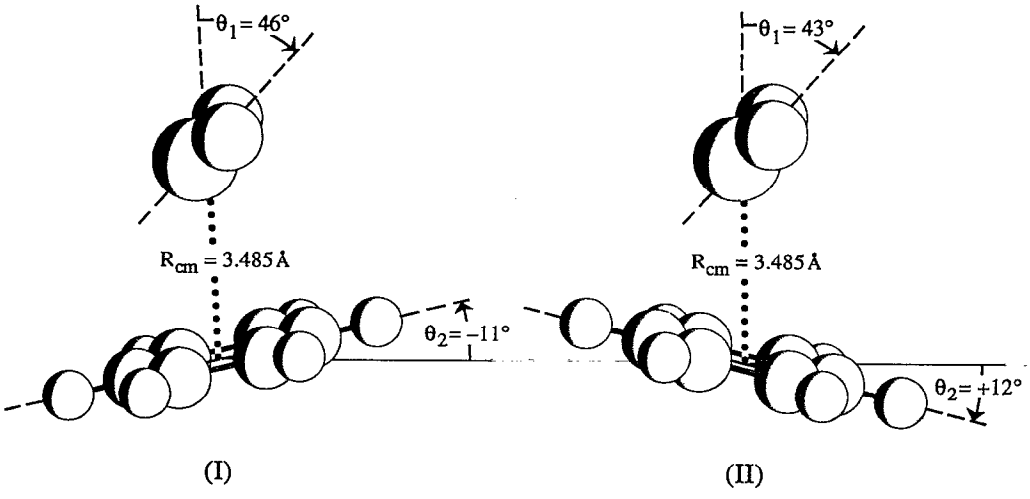

FIG. 2. The two possible structures of benzene·SO_2 consistent with fits I and II. In both figures, the *a* axis is nearly parallel to R_{cm} (dotted lines). The *ac*-plane corresponds to the plane of the page. The tilt angle θ_1 is the deviation of the C_2 axis of SO_2 from being parallel to R_{cm}, and the tilt angle θ_2 is the deviation of benzene plane from being perpendicular to R_{cm}.

accurately determined. This agreement was expected since R_{cm} is uniquely determined from the B constants[$I_b = I_a(SO_2) + I_a(\text{benzene}) + \mu(\text{benzene}\cdot SO_2)R_{cm}^2$], which is in fact unperturbed ($B=B_r$) by the internal rotation ($\theta_b = 90°$). An examination of the value of θ_1 from each fit indicates that SO_2 is tilted so that the sulfur end is pointing toward the aromatic ring. The sole difference between the structures I and II resides in the sign of θ_2. Preference of one conformation over the other cannot be made based on the quality of the least-squares fit since the ΔI_{rms} (where, $\Delta I = I_{obs} - I_{calc}$) of each fit is fairly reasonable. The calculated angles θ_a (and $\theta_c = 90° - \theta_a$) from structures in fits I and II are given in Table VIII. These calculated angles are comparable to those determined from the internal rotation fits (see Table V), and therefore, the two geometries cannot be distinguished. The dipole moment components obtained from the projection of the dipole moment of SO_2 ($\mu(SO_2) = 1.633\,05$ D[14]) onto the principal axes corresponding to each structure I and II are also listed in Table VIII. A comparison between the observed dipole moment components of benzene·SO_2 in Table VII and those obtained from the projection of $\mu(SO_2)$ shows a much better agreement with respect to μ_c than to μ_a. The relatively large discrepancy between the observed and the calculated μ_a component can be attributed mainly to the induced dipole moment arising from the large polarization of the π system along the a axis. Nevertheless, choosing between structures I and II cannot be accomplished by using this simple dipole moment analysis.

An analysis using Kraitchman's equations[30] was also undertaken with the intent to resolve the ambiguity. The substitution coordinates of oxygen were calculated using data from the single-^{18}O isotopic species, with $C_6H_6\cdot SO_2$ considered as the parent species. These substitution coordinates along with those calculated from fits I and II are listed in Table VIII. First of all, comparison between the calculated coordinates obtained from each fit shows that a difference occurs only for the c coordinate. Second, an examination of the coordinates from the Kraitchman analysis indicates that the a and b coordinates are compatible with those obtained from the fits. This supports the least-squares fit results with respect to the orientation of the tilt angle of the SO_2 monomer. Lastly, the c coordinate from fit II agrees better with the one from the Kraitchman method. However, since the difference between the c coordinates from fit I and II is not great and the rotational constants used to obtain them are still markedly affected by low frequency van der Waals vibrational modes, definitive conclusions cannot be drawn from this analysis. In fact the increase of the A rotational constant of the single-^{18}O species by 2 MHz yielded $|c(O)| = 0.167$ Å, which indicates that the preference of one conformation over the other cannot be made from the substitution analysis. Moreover, *ab initio* and electrostatic calculations are compatible with fit I. These calculations are discussed in the next section.

IV. DISCUSSION

In the present work, we successfully applied the PAM internal rotation Hamiltonian for the assignment of the torsional–rotational spectrum of benzene·SO_2. This complex displays a nearly free internal rotation of benzene about its C_6 axis. Addition of higher-order distortion terms to the PAM Hamiltonian was also necessary in fitting the spectra of benzene·SO_2. The rms error was reasonably good for the spectral fits of $C_6H_6\cdot SO_2$ ($\Delta\nu_{rms} = 48$ kHz) and $C_6D_6\cdot SO_2$ ($\Delta\nu_{rms} = 45$ kHz). Moreover, the barrier height V_6 determined for the two isotopic species, which is ~ 0.28 cm^{-1}, is in agreement with respect to the Born–Oppenheimer approximation.

Unlike other sixfold symmetry molecules whose internal rotor axis is collinear with the a axis,[17–22,25] in benzene·SO_2 the torsional–rotational spectrum was tremendously perturbed by the tilt of the C_6 axis with respect to the a (or c) axis. In fact, a characteristic of the a-dipole spectrum of molecules with a sixfold symmetry barrier and $\theta_a = 0°$, such as CH_3NO_2[17,18] and CH_3BF_2,[19] is the occurrence of bandlike series of lines centered at frequency values of $(B+C)(J+1)$. The series converge from lower and higher sides of the center frequency as m increases. However, in benzene·SO_2 the a-dipole spectrum did not show such characteristics. This made it essential to predict spectral changes quantitatively with the PAM Hamiltonian in order to assign the excited states.

To investigate the origin of the small barrier height, we employed the simple electrostatic model developed by Buckingham and Fowler.[31] The distributed multipole values for SO_2 were taken from Ref. 31. For the case of benzene, the multipoles were calculated using the distributed multipole analysis (DMA)[32] sections of the CADPAC program.[33] The distributed multipole moments for benzene are listed in Table IX; the values at the other five carbon

TABLE IX. Cartesian coordinates (in Å) and distributed multipoles (in a.u.) for benzene.[a,b,c]

Atom[d]	x	y	z	q	μ_y	Θ_{xx}	Θ_{yy}	Θ_{zz}
C(1)	0.0	−1.396	0.0	−0.035	0.088	0.118	−0.063	−0.055
H(1)	0.0	−2.479	0.0	0.035	−0.216	0.049	−0.087	0.038

[a]The distributed multipoles are calculated at the HF/6-31G** level.
[b]The energy is −230.713 01 a.u. The total charge and dipole are zero, and the total quadrupole is $\Theta_{zz}(\text{total}) = -6.337$ a.u.
[c]The following distributed multipoles are zero: μ_x, μ_z, Θ_{xy}, Θ_{xz}, and Θ_{yz}.
[d]Distributed multipoles for equivalent sites follow by symmetry.

TABLE X. Structural parameters and energies for benzene·SO_2 from *ab initio* (HF/6-31G*) calculations.[a]

	ab initio		
	$\tau = 0.0°$	$\tau = 30.0°$	Obs.[b]
R_{cm}/Å	3.732	3.737	3.485(1)
θ_1/deg	52.8	52.4	44(6)
θ_2/deg	−14.8	−14.0	±12(1)
E/a.u.	−777.875 053	−777.875 012	
E(benzene)	= −230.702 30 a.u.		
$E(SO_2)$	= −547.168 12 a.u.		

[a]Benzene and SO_2 structures were held to their uncomplexed values (Ref. 28).
[b]Structural parameters obtained from Table VIII.

and hydrogen sites can be obtained by symmetry. The structure of benzene used in the calculation of the distributed multipoles is taken from Ref. 28. Estimation of the internal rotation barrier in benzene·SO_2 using the Buckingham–Fowler model yielded $V_6=0.16$ cm^{-1}. This calculated value is surprisingly in excellent agreement with the observed value. On the other hand, an *ab initio* estimation of the barrier at the HF/6-31G* level yielded $V_6=8.9$ cm^{-1}. This barrier was calculated from geometry optimizations at two different conformations. The first conformation corresponds to the benzene torsional angle fixed at the orientation with the C_2 axis of SO_2 projected on the line joining two carbons diagonally opposite ($\tau=0.0°$), and the second one where the C_2 axis projection bisects a C–C bond ($\tau=30.0°$). The results of these calculations, which were carried out using the GAUSSIAN88 program,[34] are given in Table X. The barrier value evaluated from the *ab initio* calculations is not as close to the experimental value as that obtained from the electrostatic model. However, the experimental value is calculated assuming that R_{cm}, θ_1, and θ_2 remain unchanged while benzene is rotating about its C_6 axis, while the *ab initio* barrier is obtained from the two optimized conformations whose structural parameters R_{cm}, θ_1, and θ_2 are slightly different. Furthermore, the lack of diffuse orbitals and the neglect of electron correlation in the HF/6-31G* calculations might also lead to some error in estimating the barrier. Nevertheless, the *ab initio* value as well as the electrostatic one implies a very low barrier to internal rotation.

The assignment of the spectrum of benzene·SO_2 has shed some light on the structure of this complex. Rigid-rotor constants which are not contaminated by the internal rotation were obtained, as well as the tilt angle θ_a (or θ_2) of the benzene ring. However, experimental data needed to unambiguously determine the sign of the tilt angle θ_2 of benzene were not obtained (see Sec. III C). As mentioned above, we carried out *ab initio* geometry optimizations leading to the results in Table X. Comparing the *ab initio* structural parameters with those obtained experimentally, a fairly good agreement is seen except for R_{cm} which is off by 0.3 Å (see Table X). The sign of the *ab initio* value of θ_2 suggests that conformation I is more favorable. We have also carried out electrostatic calculations using the Buckingham–Fowler model to derive the electrostatic energies of conformations I and II listed in Table VIII. Values of -2.0 and -1.6 kcal mol^{-1} were obtained for I ($\theta_2=-11°$) and II ($\theta_2=+12°$), respectively. This suggests that the conformation where $\theta_2=-11°$ is more stable, which is compatible with the *ab initio* results. Although the electrostatic and *ab initio* calculations seem to favor the conformation from fit I ($\theta_2=-11°$), this cannot be taken as definitive. This is because for weakly bound complexes, *ab initio* calculations beyond the HF level are needed to accurately model the interaction energy and reasonably reproduce the experimental structure. Similar caution is warranted for the electrostatic model since here the difference of energy between the two conformations is small (0.4 kcal mol^{-1}), the repulsive term is not quantitatively incorporated, and additional terms such as dispersion, polarization, and charge transfer are necessary to more reliably estimate energy differences.

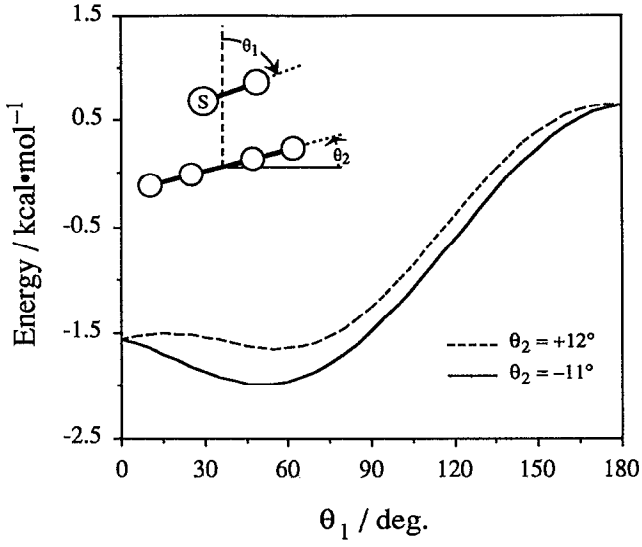

FIG. 3. Electrostatic interaction energy as a function of the tilt angle, θ_1, of SO_2. The solid line and dashed line plots correspond to the tilt angle, θ_2, of benzene fixed at $-11°$ (fit I) and $+12°$ (fit II), respectively. The sign convention for θ_2 is consistent with that in Fig. 2.

This preference for the negative θ_2 is, of course, compatible with the inertial data (see above) which is ambiguous regarding the sign of this angle. Although perhaps not relevant, it is also interesting that a negative tilt angle is observed for ethylene in ethylene·SO_2.[35(a)] It may be possible to unambiguously determine the sign of θ_2 experimentally from rotational constants for a benzene·SO_2 species containing an asymmetric deuterium species.

The Buckingham–Fowler model was used to see if electrostatic interactions can account for the observed tilt angle θ_1 of the SO_2 subunit. This model was previously applied to ethylene·SO_2,[35(a)] acetylene·SO_2,[35(b)] and furan·SO_2.[36] In these complexes the observed tilt angle of SO_2 and that obtained from the electrostatic model were in fairly good agreement. The electrostatic energy calculated as a function of θ_1 is shown in Fig. 3. In this figure, the dashed line and the solid line plots correspond to the energy calculated with the benzene plane held fixed at $\theta_2=+12°$ and $-11°$, respectively. R_{cm} was fixed at the observed value of 3.485 Å. Examination of Fig. 3 shows that the shallow minima obtained around $\theta_1=45°$–$60°$ are consistent with the experimental geometry. This agreement is pleasing since it follows simple intuition suggesting an interaction between the positive sulfur and the benzene π cloud.

Finally, the binding energy for the experimental geometry of benzene·SO_2 obtained from the electrostatic and *ab initio* calculations (from Table X) are 2.0 and 2.9 kcal mol^{-1}, respectively. The observed D_J and pseudodiatomic approximation,[37] yielded a value of 1.9 kcal mol^{-1} for the binding energy. These values are somewhat smaller than the experimental value 4.4(3) kcal mol^{-1} measured by

Grover *et al.*[5] A similar large underestimate of the binding energy using the pseudodiatomic approximation was observed for the even stronger complex between trimethylamine and SO_2.[38]

ACKNOWLEDGMENTS

The authors acknowledge the assistance of Dr. Marabeth S. LaBarge who first cataloged some of the strong excited torsional state lines into series. The work was supported by the Experimental Physical Chemistry Program, National Science Foundation, Washington D. C. The authors are grateful to the Donors of the Petroleum Research Fund, administered by the American Chemical Society for the support of this work in the form of fellowship stipends to ATB. An allotment of computing time for calculations on the San Diego Supercomputer facility is gratefully acknowledged.

[1] L. J. Andrews and R. M. Keefer, J. Am. Chem. Soc. **73**, 4169 (1951).
[2] P. A. D. de Maine, J. Chem. Phys. **26**, 1036 (1957).
[3] D. Booth, F. S. Dainton, and K. J. Ivin, Trans. Faraday Soc. **55**, 1293 (1959).
[4] B. C. Smith and G. H. Smith, J. Chem. Soc. **1965**, 5514.
[5] J. R. Grover, E. A. Walters, J. K. Newman, and M. G. White, J. Am. Chem. Soc. **107**, 7329 (1985).
[6] M. S. LaBarge, J. J. Oh, K. W. Hillig II, and R. L. Kuczkowski, Chem. Phys. Lett. **159**, 559 (1989).
[7] (a) A. J. Gotch and T. S. Zwier (private communication); (b) A. J. Gotch, A. W. Garrett, D. L. Severance, and T. S. Zwier, Chem. Phys. Lett. **178**, 121 (1991).
[8] (a) A. Engdahl and B. Nelander, J. Phys. Chem. **89**, 2860 (1985); (b) **91**, 2253 (1987).
[9] Th. Weber, A. M. Smith, E. Riedle, H. J. Neusser, and E. W. Schlag, Chem. Phys. Lett. **175**, 79 (1990).
[10] Y. Ohshima, H. Kohguchi, and Y. Endo, Chem. Phys. Lett. **184**, 21 (1991).
[11] C. A. Fyfe, *Molecular Complexes*, edited by R. Foster (Elek Science, London, 1973), Vol. 1, p. 209.
[12] K. W. Hillig II, J. Matos, A. Scioly, and R. L. Kuczkowski, Chem. Phys. Lett. **133**, 359 (1987).
[13] R. K. Bohn, K. W. Hillig II, and R. L. Kuczkowski, J. Phys. Chem. **93**, 3456 (1989).
[14] D. Patel, D. Margolese, and T. R. Dyke, J. Chem. Phys. **70**, 2740 (1979).
[15] H. C. Longuet-Higgins, Mol. Phys. **6**, 445 (1963).
[16] P. R. Bunker, *Molecular Symmetry and Spectroscopy* (Academic, New York, 1979).
[17] E. Tannenbaum, R. J. Myers, and W. D. Gwinn, J. Chem. Phys. **25**, 42 (1956).
[18] F. Rohart, J. Mol. Spectrosc. **57**, 301 (1975).
[19] R. E. Naylor and E. B. Wilson, Jr., J. Chem. Phys. **26**, 1057 (1957).
[20] W. M. Tolles, E. T. Handelman, and W. D. Gwinn, J. Chem. Phys. **43**, 3019 (1965).
[21] T. Ogata, A. P. Cox, D. L. Smith, and P. L. Timms, Chem. Phys. Lett. **26**, 186 (1974).
[22] P. R. R. Langridge-Smith and A. P. Cox, J. Chem. Soc. Faraday Trans. 2 **79**, 1089 (1982).
[23] C. C. Lin and J. D. Swalen, Rev. Mod. Phys. **31**, 841 (1959).
[24] P. A. Helminger and F. C. DeLucia, J. Mol. Spectrosc. **111**, 66 (1985).
[25] (a) H. D. Rudolph, H. Dreizler, A. Jaeschke, and P. Wendling, Z. Naturforsch. Teil A **22**, 940 (1967); (b) H. D. Rudolph and H. Seiler, *ibid.* **20**, 1682 (1965); (c) H. D. Rudolph, H. Dreizler, and H. Seiler, *ibid.* **22**, 1738 (1967).
[26] J. K. G. Watson, *Vibrational Spectra and Structure*, edited by J. R. Durig (Elsevier, Amsterdam, 1977), Vol. 6, Chap. 1.
[27] J. K. G. Watson, J. Chem. Phys. **46**, 1935 (1967).
[28] M. D. Harmony, V. W. Laurie, R. L. Kuczkowski, R. H. Schwendeman, D. A. Ramsey, F. J. Lovas, W. J. Lafferty, and A. G. Maki, J. Phys. Chem. Ref. Data **8**, 619 (1979).
[29] R. W. Kilb, C. C. Lin, and E. B. Wilson, Jr., J. Chem. Phys. **26**, 1695 (1957).
[30] J. Kraitchman, Am. J. Phys. **21**, 17 (1953).
[31] A. D. Buckingham and P. W. Fowler, Can. J. Chem. **63**, 2018 (1985).
[32] A. J. Stone, Chem. Phys. Lett. **83**, 233 (1981).
[33] R. D. Amos and J. E. Rice, Cambridge Analytical Derivatives Package (CADPAC), issue 4.0, 1987.
[34] M. J. Frisch, M. Head-Gordon, H. B. Schlegel, K. Raghavachari, J. S. Binkley, C. Gonzalez, D. J. Defrees, D. J. Fox, R. A. Whiteside, R. Seeger, C. F. Melius, J. Baker, R. L. Martin, L. R. Kahn, J. J. P. Stewart, E. M. Fluder, S. Topiol, and J. A. Pople, GAUSSIAN88 (Gaussian, Inc., Pittsburgh, PA, 1988).
[35] (a) A. M. Andrews, A. Taleb-Bendiab, M. S. LaBarge, K. W. Hillig II, and R. L. Kuczkowski, J. Chem. Phys. **93**, 7030 (1990); (b) A. M. Andrews, K. W. Hillig II, R. L. Kuczkowski, A. C. Legon, and N. Howard, *ibid.* **94**, 6947 (1991).
[36] J. J. Oh, L.-W. Xu, A. Taleb-Bendiab, K. W. Hillig II, and R. L. Kuczkowski, J. Mol. Spectrosc. **153**, 497 (1992).
[37] D. J. Millen, Can. J. Chem. **63**, 1477 (1985).
[38] J. J. Oh, Marabeth S. LaBarge, J. Matos, J. W. Kampf, K. W. Hillig II, and R. L. Kuczkowski, J. Am. Chem. Soc. **113**, 4732 (1991).